İSTANBUL UNIVERSITY CERRAHPAŞA

ORIGINAL ARTICLE
Electrica 2023; 23(3): 414-428

Application of Fuzzy Proportional Integral Derivative Controller in Automatic Generation Control Using Hybrid African Vultures Optimization Algorithm-Pattern Search Optimization Algorithm for Frequency Control of Power System with Electric Vehicles

Pabitra Mohan Dash[1], Asini Kumar Baliarsingh[2], Sangram Keshori Mohapatra[3]

[1]Department of Electrical Engineering, BEC, Bhubaneswar, Odisha, India
[2]Department of Electrical Engineering, GCE, Kalahandi, Odisha, India
[3]Department of Electrical Engineering, GCE, Keonjhar, Odisha, India

Cite this article as: P. Mohan Dash, A. Kumar Baliarsingh and S.K. Mohapatra, "Application of fuzzy proportional integral derivative controller in automatic generation control using hybrid African vultures optimization algorithm-pattern search optimization algorithm for frequency control of power system with electric vehicles," *Electrica*, 23(3), 414-428, 2023.

ABSTRACT

In the continually increasing size and configuration of the modern power system with unpredictable load and integration of electric vehicles (EVs), the usage of intelligent and effective scheme is essential to control system frequency. This work suggests a hybrid African vultures optimization algorithm (AVOA) and pattern search (hAVOA-PS)-based fuzzy proportional integral derivative (FPID) structure for frequency control of a nonlinear power system with EVs. To illustrate the dominance of the projected hAVOA-PS algorithm, initially, PI controllers are considered and results are equated with AVOA, particle swarm optimization, and genetic algorithm methods. To further enhance the dynamic performance, PID and FPID controllers are considered. The dominance of FPID over PID and PI controllers is shown. In the next step, EVs are integrated into the test system and a comparative investigation of hAVOA-PS-based PI/PID/FPID and FPID+EV is presented. To exhibit the superiority of projected frequency control scheme in maintaining the stability of system under different disturbance conditions like load increase in area-1 only, load decrease/increase in all areas and large load increase in all areas are considered. It is noticed that the proposed hAVOA-PS-based FPID controller in the presence of EV is able to maintain system stability for all the considered cases, whereas other compared approaches fail to maintain stability in some cases. The effectiveness of the projected frequency control method is equated with some recently suggested approaches in a standard two-area system. At last, MATLAB results are equated with Open Real-Time Digital Simulators (OPEN-RT) outcomes to validate the feasibility and effectiveness of the proposed scheme for practical applications

***Index Terms*—**African vultures optimization algorithm, automatic generation control, fuzzy proportional integral derivative controller, electric vehicles, pattern search

Nomenclature

AGC	Automatic Generation Control	ΔF_i	Change in area frequency, Hz
i	Control area number	*GDB*	Governor Dead Band
P_{ri}	Rating of area i, MW	*GRC*	Generation Rate Constraint
R_i	Regulation index of the Governor, Hz/pu	J_s	Performance index
β_i	Frequency bias, pu/Hz	U_S/O_S	Undershoot/Overshoot, p.u.
K_{Psi}	Power system gain, Hz/pu	*PID*	Proportional Integral Derivative
T_{Psi}	Power system time constant, s.	*FLC*	Fuzzy Logic Control
T_{Gi}	Time constant of governor, s.	*FPID*	Fuzzy PID
T_{Ti}	Time constant of turbine, sec.	*MFs*	Membership functions
T_{12}	Synchronizing coefficient of tie-line, s	*SF*	Scaling factor
ΔP_{Ci}	Controller output	*GA*	Genetic Algorithm
ACE_i	Area control error	*PSO*	Particle Swarm Optimization
ΔP_{Li}	Load demand change, pu	*AVOA*	African Vultures Optimization Algorithm
ΔP_{tieij}	Tie-line power change, pu	*PS*	Pattern Search
ITAE	Integral Time Absolute Error	*hAVOA-PS*	Hybrid AVOA PS
		EV	Electric Vehicle

Corresponding author:
Sangram Keshori Mohapatra

E-mail:
sangram.muna.76@gmail.com

Received: July 22, 2022

Accepted: October 31, 2022

Publication Date: August 1, 2023

DOI: 10.5152/electrica.2023.22124

I. INTRODUCTION

In an interconnected power system, unsystematic variations in load cause the tie-line power and frequency to diverge from their nominal values. To maintain equilibrium between frequency and generation, an automatic control system is essential. The automatic generation control (AGC) scheme in the power system reduces the frequency and tie-line power deviations by properly varying the generations [1].

A. Literature Review

Many investigators have applied several secondary controllers in the AGC system such as conventional controller, proportional integral derivative (PID) controller in AGC of diesel/wind turbine generators [2], the AGC studies has been attempted the bacterial foraging (BF) based optimal design of integral plus double derivative controllers and fuzzy based Integral Double Derivative (IDD) controller structures of the system, two degrees of freedom controller (2DOF) effectively implemented in the multi-microgrid system in [3]. In AGC study, different type of advanced controller like sliding mode controller has been analyzed the frequency regulation in nonlinear power systems [4], modified equilibrium optimization tune multistage PID have been carried out in AGC systems [5]. The effect of wind power was also analyzed for AGC in the interconnected power system. Frequency regulation for a hybrid distributed power system by tilted PID has been done in [6]. Grasshopper optimization algorithm (GOA)-tuned multistage fractional proportional derivative (PDF)+(1+PI) structure has been studied for AGC issues with flexible AC transmission systems (FACTS) controller. The influence of various energy storage (ES) components with cascade controllers to mitigate the frequency oscillations has been studied in [7]. To observe the disturbance due to boiler dynamics in the thermal unit and wind power penetration, a sunflower optimization-based multistage fuzzy controller has been introduced for frequency regulation in [8]. The impact of H_2 equalizer-based fuel cell in AGC using fuzzy fractional order controller has been introduced in [9].

For solving the AGC problem, researches are attempted in the AGC studies in different power system for the optimal tuning of PI controllers with the BAT algorithm for frequency stability analysis. A combined analysis of genetic algorithm (GA) and particle swarm optimization (PSO)-tuned fuzzy system has been studied in a nonlinear power system. The hybridization of the multi-verse (MVO) and pattern search (PS) method is engaged in the load frequency control (LFC) of interconnected system. Bacteria foraging optimization algorithm-based fractional order fuzzy set has been tested for AGC in multi-area multi-source power system. Hybrid differential evolution (DE)-PSO algorithm is applied to set fuzzy variables in AGC study in [4]. The design and application of the PID controller have been analyzed for real-type validation in the power system. The concept of fuzzy logic controllers (FLCs) with ES has been applied in the AGC study. Frequency control of a practical power system with different types of generation has been studied. The rule-based fuzzy controller is studied in [4]. The PID controller with an adaptive fuzzy structure has been carried out to control nonlinear processes in [4]. These are the different studies for solving AGC problems attempted by researchers for interconnection of multi-area power system.

Recently, novel optimization approaches have been applied to many controller design problems for frequency control. A quasi oppositional Jaya-tuned two-degree of freedom PID has been projected for a two-area system including the nonlinearities in [10]. A sine logistic map based chaotic sine cosine algorithm tuned proportional integral derivative (PID) controller for frequency regulation of a microgrid with photovoltaic system (PV), wind, fuel cell, battery energy storage system (BESS), flywheel energy storage system (FESS), diesel engine generator (DEG), and micro turbine (MT) has been attempted in AGC studies of the power system [11]. A 2DOF-tilted integral derivative with filter tuned by bat and harmony search algorithm has been proposed for two-area wind-hydro-diesel units with superconducting magnetic energy storage (SMES) and FACTS devices [12]. In [13], a PDF-PI structure tuned by coyote optimization was suggested for frequency regulation of a two-area system with wind, PV, and gas turbine sources. A chaotic atom search optimization-based fractional order proportional-integral-derivative (FOPID) structure for frequency regulation of a hybrid system was presented in [14]. Mayfly optimization-tuned fuzzy PD-(1+I) configuration was recommended in [15] for a microgrid containing solar–thermal, wind, micro-hydro turbine, biodiesel, and biogas generators. Atom search optimization and grey wolf optimization (GWO)-based FOPID controllers have been suggested to control the frequency of hybrid power system containing plug-in electric vehicle (PEV), wind turbine power generation (WTPG), solar thermal power generation (STPG), and thermal units considering nonlinearities [16]. A fuzzy gain scheduling controllers are suggested for AGC of power systems [17] where the controller parameters are tuned by genetic algorithm. An AGC scheme by a layered recurrent artificial neural network is projected in [18] for AGC of nonlinear power system. A slap swarm algorithm-optimized FPID structure with redox flow battery is proposed in [19] to regulate the frequency of a realistic power system. A fuzzy PID structure optimized with coyote optimization algorithm is suggested in [20] for a doubly fed induction generator-integrated power system. An fuzzy PID structure optimized by glow-worm swarm optimization [21], hybrid local unimodal sampling–teaching learning-based optimization [22], etc. have also been reported in literature. A fuzzy PD+I structure for frequency control of renewable power integrated with demand response supported isolated hybrid microgrid has been reported in [23].

B. Research Gap and Motivation

The study of recent articles based on AGC problems confirms that various combined efforts of control approaches along with optimizing tools are successfully interfaced with some power grid models to get improved solutions. But no particular approach cannot give satisfactory results for all types of problems. Therefore, this is an opportunity to explore alternative approaches by suggesting novel robust control schemes. African vultures optimization algorithm (AVOA) is a lately offered optimization method motivated by the African vultures' navigation and foraging characteristics [24]. The dominance of AVOA over GWO, PSO, fire fly algorithm (FFA), whale optimization algorithm (WOA), moth-flame optimization (MFO), teaching learning-based optimization (TLBO), differential evolution (DE), biogeography-based optimization (BBO), gravitational search algorithm (GSA), salp swarm algorithm (SSA), and input–process–output (IPO) has been demonstrated using benchmark test functions. However, effectiveness of AVOA over other similar techniques in controller design problem has not been reported. Also, AVOA is a global search technique that looks at the broad search area and may not be effective if employed unaided. Conversely, PS which is a local search method searches the local area but is not effective for wider search [3]. In consequence of their strengths, these two methods can be mixed to get improved performance. Therefore, a

hybrid AVOA-PS method is projected in this paper for tuning fuzzy PID (FPID) parameters for frequency control of power system. The main contribution of this research work to overcome the weakness is recognized in the performance of the normal version of the AVOA: local optima trapping and minimal population diversity which results in premature convergence. Because of this lacking, AVOA needs to be improvised or hybridized with other techniques or local search optimizations. The improvement in performance is noticed, by hybridizing the normal AVOA and PS algorithm called hAVOA-PS.

C. Contribution

The novel contributions of the present study are:

- To propose a new nature-inspired evolutionary hybridized AVOA and PS (hAVOA-PS) technique to design a fuzzy-PID (FPID) controller for frequency control of a five-area nonlinear power system in the presence of electric vehicle (EV).
- To demonstrate the supremacy of the projected algorithm (hAVOA-PS); it is related to other conformist techniques like GA, PSO, and AVOA and proposed control scheme (FPID with EV) over FPID without EV as well as PID and PI controllers.
- To show the superiority of projected frequency control scheme in maintaining the stability of system under different disturbance conditions like load increase/decrease in one/all areas, large load increase in all areas, and parameter variation condition.
- To compare the usefulness of the suggested frequency control method with some published approaches in a standard two-area system.
- To validate the proposed approach, MATLAB results by comparing with OPAL results.

D. Paper Organization

The study is structured as follows: Section II describes the test system, Section III discusses the controller structure and objective function, Section IV enlightens the overview of hAVOA-PS, Section V provides the results and discussions, and Section VI summarizes the conclusion.

II. TEST SYSTEM

With the growing demand for EVs, it is expected that EVs will be extensively used in future power systems. EVs give a prospect to employ their batteries during plug-in; considering a fleet of EVs, they could act as an ancillary facility for the future power system. It is therefore necessary to evaluate the capability of EVs in frequency control of studied system. An interconnected thermal power system consisting of five areas is taken as test system. Figure 1 shows the transfer function model of one area with EV. The figure presentation modeling of EV for frequency control is also demonstrated in Fig. 1 [16]. The LFC signal ΔU is supplied to EV for discharging/charging. Parameters $\pm BkW$ signify the battery capacity. The existing battery energy is signified by E that is kept inside the restrictions $E_{\max}$ and $E_{\min}$ presumed as 90% and 60%. K_1 and K_2 are found as $K_1 = E - E_{\max}$, $K_2 = E - E_{\min}$. The stored energy part in Fig. 1 computes the remaining stored energy.

The complete five-area system is revealed in Fig. 2. The ratings are 2000 MW, 4000 MW, 8000 MW, 10 000 MW, and 12 000 MW, respectively, for areas 1–5. The system data are taken from [2]. For dissimilar rating (P_{Ri} and P_{Rj}) of areas i and j, a factor $a_{ij} = -P_{Ri}/P_{Rj}$, is employed to characterize the values in p.u. In frequency control studies, it is important to study the elementary physical constraints and take account of them to get an appropriate knowledge of the frequency control issues. The main constraints are generation rate constraint (GRC) and governor dead band (GDB) nonlinearity which is taken as 3%/min and 0.036 Hz, respectively [2]. The information offered by Fosha and Elgerd [1] is referred to for developing the system model.

III. CONTROLLER STRUCTURE AND OBJECTIVE FUNCTION

Proportional integral (PI) controllers are generally employed in control systems for their modest design, less cost, and their practicality for linear systems. However, traditional PI structures are usually not competent for nonlinear systems. On the other hand, FLC is flexible, simple to understand, and implement. It helps to follow the human thought logic. It is a very appropriate scheme for uncertain and

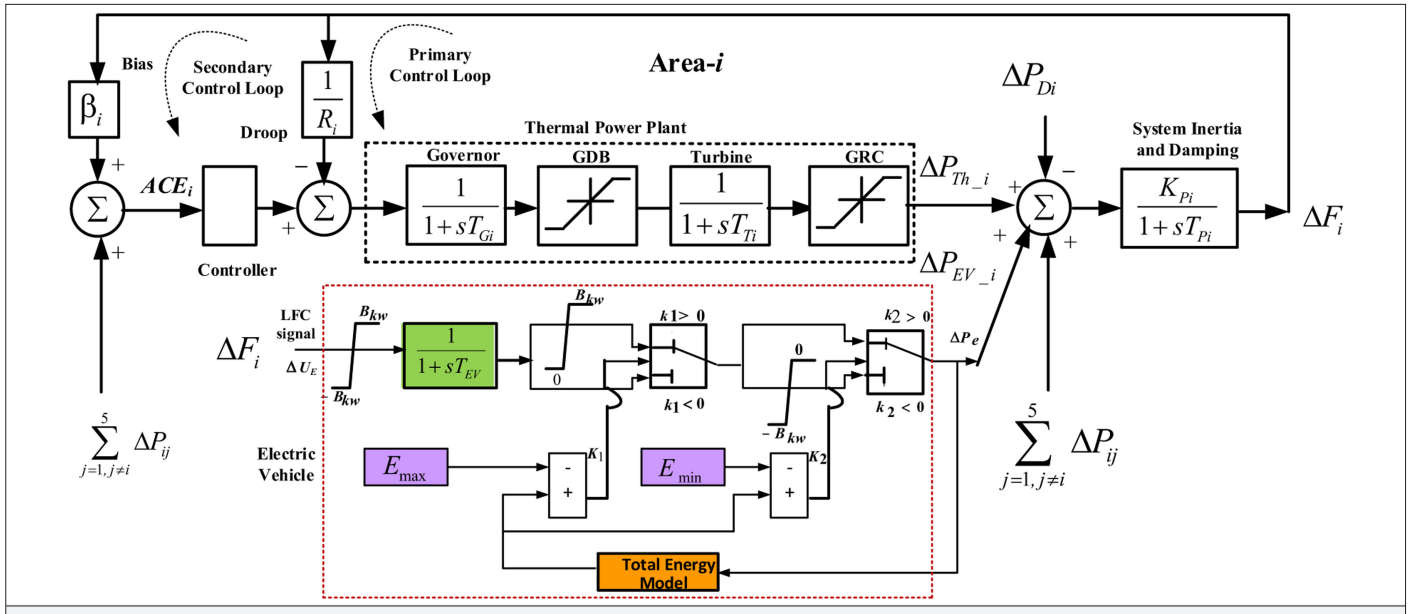

Fig. 1. Transfer function model of *i*th area with EVs.

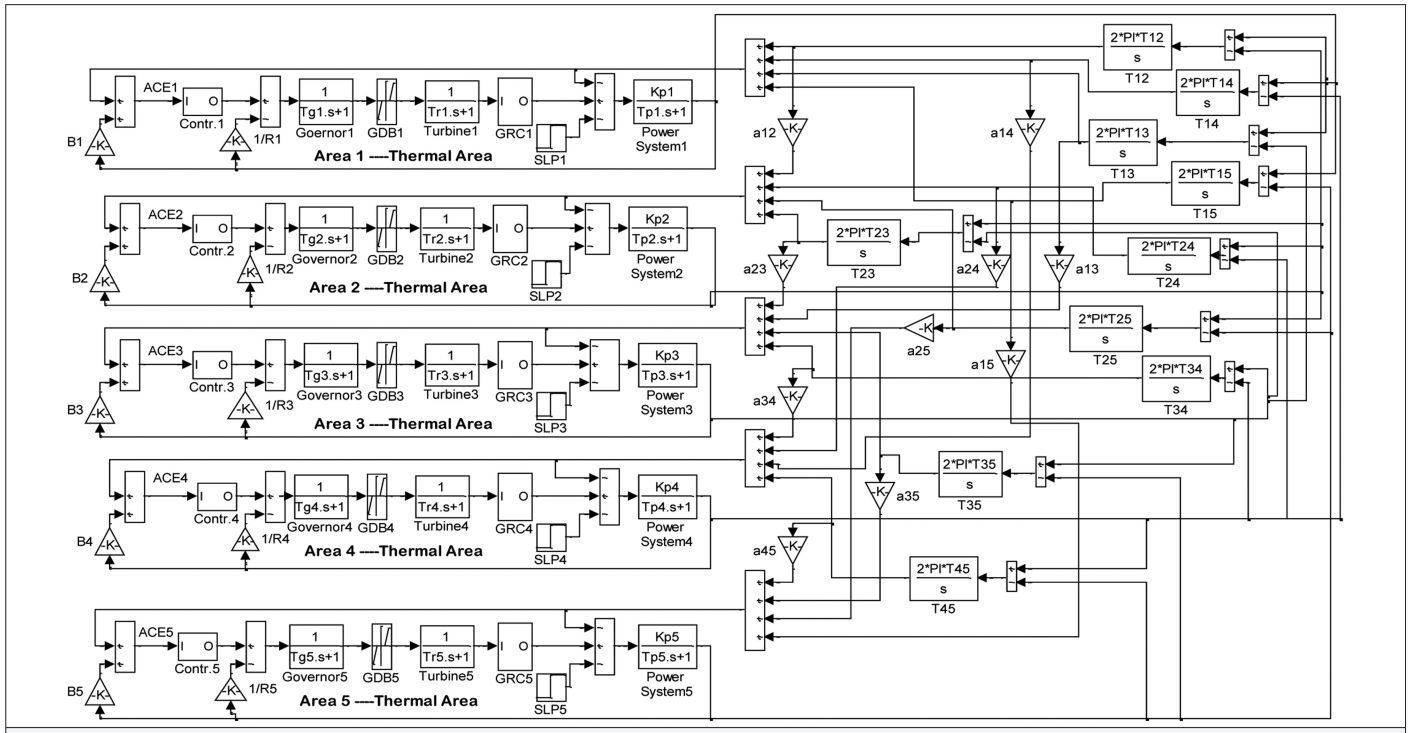

Fig. 2. Five-area system under investigation.

approximate reasoning. Therefore, the system performance can be enhanced by employing an FPID controller.

An FLC-based PI (FPI) structure increases the system performance as FLC can deal with nonlinearity [3]. Design of an appropriate FLC involves choice of appropriate membership functions (MFs) and construction of rules which is a difficult job. Conversely, common rule base and MFs can be selected and the scaling factors (SFs)/PI parameters can be optimized for satisfactory operation. Nevertheless, the FPI configuration might yield unacceptable system performance in initial periods for nonlinear systems due to its intrinsic integral act. To overcome this, a derivative component is added resulting in FPID controller [9]. Therefore, an FPID controller revealed in Fig. 3 is selected in this study for frequency control. Individual area control errors and their derivatives are passed through SFs (K_1 and K_2) and given as inputs to FPID. The FLC output is passed through a PID controller where K_P, K_I, and K_D are the PID parameters. The FPID outputs manage the powers of specific generating units.

A. Fuzzy Logic Controller Design

Usually triangular MFs are favored as their real-world execution can simply be attained. They also require lowest storage obligation and can be functioned economically to meet stiff real-time necessities. Same MFs for inputs/output are typically preferred from computational adeptness viewpoint in addition to memory management ability [25]. Thus, similar MFs are chosen for the input/output of FLC. The linguistics negative big (NB), negative small (NS), zero (Z), positive small (PS), and positive big (PB) are used as illustrated in Fig. 4. Mamdani's and center of gravity methods are chosen as fuzzy interface engine and defuzzification method. The rule base is shown in Table I.

For optimization technique-based controller design, the objective function (J) is usually stated based on some performance measures. The J is formulated keeping in mind the desired control specifications. Various criteria such as integral time absolute error (ITAE), integral squared error (ISE), integral absolute error (IAE), and integral

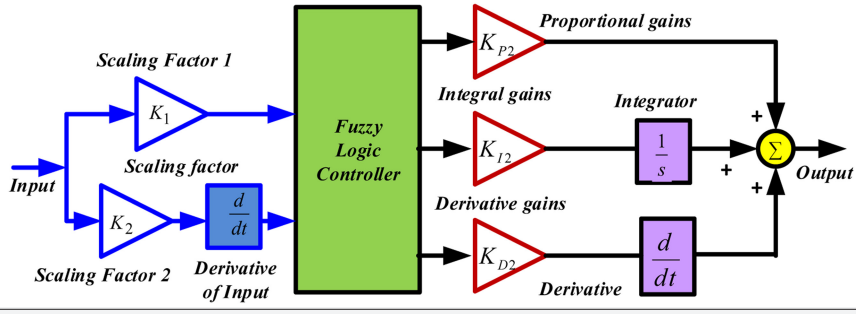

Fig. 3. Fuzzy PID (FPID) configuration [9].

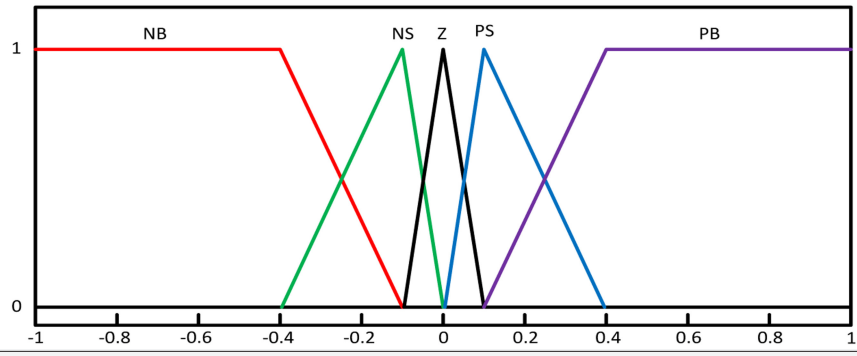

Fig. 4. MFs of error and change of error of FPID [9].

TABLE I. RULE BASE FOR ERROR, DERIVATIVE OF ERROR, AND FLC OUTPUT [9]

			de/dt		
e	**NB**	**NS**	**Z**	**SP**	**LP**
NB	NB	NB	NS	NS	Z
NS	NB	NS	NS	Z	PS
Z	NS	NS	Z	PS	PS
PS	NS	Z	PS	PS	PB
PB	Z	PS	PS	PB	PB

FLC, fuzzy logic controllers.

time squared error (ITSE) have engaged in literature [3-7]. It has also been demonstrated in numerous works that ITAE criteria offer improved system performance related to others.

An ITAE criterion specified in (1) is selected as it yields minimum over shoots (OS) and settling times related to other measures like ISE, IAE, ITSE, and ISTE.

$$J = ITAE = \int_0^t \left(\left|\Delta F_i\right| + \left|\Delta P_{Tie-i}\right|\right) \cdot t \cdot dt \tag{1}$$

where ΔF_i and ΔP_{Tie-i} are frequency and tie-line power deviation in *i*th area, respectively, and t is simulation time.

IV. HYBRID AFRICAN VULTURES OPTIMIZATION ALGORITHM AND PATTERN SEARCH

A. African Vulture Optimization Algorithm

AVOA is a new population-based search algorithm proposed in year 2021 [24]. The algorithm is motivated by way of life, food explore, and struggle for food by different vultures in Africa. In AVOA, a balance between diversity and quality is formed by the employing two best solutions in AVOA. The four stages of AVOA algorithms are:

1) Finding the Best Vulture: First Stage

After initialization, the fitness of every candidate is found, and the first and second best solutions are chosen as the two best candidates. The remaining candidates shift toward these best solutions as per (2)

$$R(i) = \begin{Bmatrix} Best\ Vulture_1 & if\ p_i = L_1 \\ Best\ Vulture_2 & if\ p_i = L_2 \end{Bmatrix} \tag{2}$$

In (2), the probability of selecting the particular vultures is determined using (3), that is, Roulette wheel, where L_1 and L_2 vary between 0 and 1 and their sum is 1. If one parameter is close to 1, then the other parameter will be close to 0 causing increased intensification. The reverse values result in increased diversification.

$$pi = \frac{F_i}{\sum_{i=1}^{n} F_i} \tag{3}$$

2) Starvation Rate of Vultures: Second Stage

Vultures look out for food at all times and have a sufficient energy when they are satiated, allowing them to look for food at larger distances, but when they are hungry, they do not have the energy to fly. This is mathematically expressed in (4).

$$F = \left(2 \times rand_1 + 1\right) \times z \times \left(1 - \frac{IT_i}{IT_M}\right) + t \tag{4}$$

where

$$t = h \times \left(\sin\left(\frac{\pi}{2} \times \frac{IT_i}{IT_M}\right)^{\gamma} + \cos\left(\frac{\pi}{2} \times \frac{IT_i}{IT_M}\right) - 1\right) \tag{5}$$

In above equations, F signifies the satisfactions, IT_i and IT_M indicate the current and max iterations, respectively; $rand_1$, z, and h are arbitrary values between (0 to 1), (−1 to 1), and (−2 to 2). When the z value falls below zero, the vulture is starving; when it increases to zero, the vulture is satiated.

There is no assurance that the finishing solutions will contain correct approximations of the global best at the conclusion of the exploration stage when addressing difficult optimization issues. As a result, it results in an early convergence at the best local site. Equation (4) is utilized to improve effectiveness while solving difficult optimization tasks, which results in a higher degree of dependability for escape from local optimal spots. The AVOA algorithm's final iterations execute the exploitation stage and, in some cases, exploration activities. The overall objective of this technique is to adjust (5) to switch between the exploration and exploitation stages, hence increasing

the chance of the AVOA algorithm performing the exploration stage sometime during the search procedure. In (4), "sin" and "cos" denote the sine and cosine functions, respectively. The parameter "w" is a fixed-value set prior to the search process that specifies whether the search process disturbs the exploration and operation stages; increasing the "w" parameter enhances the probability of performing the exploration stage in the later search process.

The total number of vultures is decreasing, and the rate of decline is increasing with each repeat. When |F| exceeds 1, vultures begin hunting for food in new sites, initiating the exploration phase of the AVOA. If |F| <1, AVOA initiates the exploitation stage, during which vultures begin seeking food in nearby areas.

3) Exploration: Third Stage

In this stage, the vultures have extraordinary vision and an incredible capability to seek food and identify dead animals in their native habitat. Vultures, on the other hand, occasionally face food shortages. Vultures spend considerable time inspecting their surroundings and cover enormous path in search of food. Vultures can use one of two separate techniques to investigate different random sites inside the AVOA, and a factor called P_1 is employed for selecting which scheme to apply. This parameter has a worth between 0 and 1, influencing how each of the schemes is followed.

To choose any of the schemes in the $rand_{P1,}$ exploration stage, an arbitrary value between 0 and 1, is created. The vulture location in next iteration is calculated as:

$$P(i+1)=\begin{Bmatrix} Equation(7) & if\ p_i \geq rand_{P1} \\ Equation(9) & if\ p_i < rand_{P1} \end{Bmatrix} \tag{6}$$

$$P(i+1)=R(i)-D(i)\times F \tag{7}$$

$$D(i)=\left|X\times R-D(i)-P(i)\right| \tag{8}$$

In (7), vultures arbitrarily look for food in the nearby region within a haphazard distance of one of the two groups' greatest cultures. In above equations, $P(i)$ and $P(i+1)$ are the vulture location vector in the present and next iterations and F is the vulture satiation rate in the present iteration; R(i) is one best vulture, as determined by the current iteration's usage of (2). Additionally, X is the location of vultures that fly randomly in order to guard food from several vultures and is found by $X = 2 \times rand$, where rand is an arbitrary value between 0 and 1. $P(i)$ is the present vector location of the vulture.

$$P(i+1)=R(i)-F+rand_2\times\left((ub-lb)\times rand_3+lb\right) \tag{9}$$

where $rand_2$ and $rand_3$ are random values in the limit 0 and 1, lb and ub are the bound of the variables.

4) Exploitation: Fourth Stage

In this stage, if $|F| <1$, the AVOA performs exploitation in two phases with different schemes. The factors P_2 and P_3 are employed to choose the schemes available in the first and second stages. Both P_2 and P_3 lie between 0 and 1.

Exploitation: The algorithm performs the first step in the exploitation stage if $|F|$ lies between 1 and 0.5. Here, two diverse rotating flight and siege-fight schemes are executed as given in (10):

$$P(i+1)=\begin{Bmatrix} Equation(11) & if\ p_i \geq rand_{P2} \\ Equation(14) & if\ p_i < rand_{P2} \end{Bmatrix} \tag{10}$$

Competition for Food: If $|F| = 0.5$, vultures are reasonably satisfied and have enough supply of energy. When a large number of vultures concentrate around a single food supply, serious fights over food acquisition can occur. In such situations, physically powerful vultures do not wish to share the food, but the weaker ones attempt to exhaust the strong vultures and get food from them by congregating around robust vultures and instigating trivial fights. This is replicated using (11) and (12).

$$P(i+1)=D(i)\times(F+rand_4)-d(t) \tag{11}$$

$$d(t)=R(i)-P(i) \tag{12}$$

$D(i)$ is evaluated by (8), $rand_4$ is a four-digit arbitrary value between 0 and 1

Vultures rotating flight: Vultures are known for their rotating flying representing spiral movement. In this procedure, a spiral expression is generated among all vultures. Equations (12) and (13) are used to express circular flight (13).

$$S_1=R(i)\times\left(\frac{rand_5\times P(i)}{2\pi}\right)\times\cos\left(P(i)\right) \tag{13}$$

$$S_2=R(i)\times\left(\frac{rand_6\times P(i)}{2\pi}\right)\times\sin\left(P(i)\right) \tag{14}$$

$$P(i+1)=R(i)-(S_1+S_2) \tag{15}$$

R(i) indicates the location vector of one best vultures in the present iteration. And $rand_5$ and $rand_6$ are random numbers ranging from 0 to 1. Here, S1 and S2 are calculated using (13). Finally, the position of the vultures is reorganized using (14).

5) Second Exploitation Stage

In this stage, if $|F| < 0.5$, the two vultures' travels gather some more vultures near food, and the blockade and hostile conflict to locate food are performed. This process is revealed as

$$P(i+1)=\begin{Bmatrix} Equation(17) & if\ p_3 \geq rand_{P3} \\ Equation(18) & if\ p_3 < rand_{P3} \end{Bmatrix} \tag{15}$$

Gathering of vultures near food: Sometimes, if vultures are hungry, several vultures gather near the food. This process is revealed as:

$$A_1=Best\ Vulture_1(i)-\frac{Best\ Vulture_1(i)\times P(i)}{Best\ Vulture_1(i)-P(i)^2}\times F$$

$$A_2=Best\ Vulture_2(i)-\frac{Best\ Vulture_2(i)\times P(i)}{Best\ Vulture_2(i)-P(i)^2}\times F \tag{16}$$

In (16), $BestVulture_1(i)$ and $BestVulture_2(i)$ are the best vulture of the first and second group in the present iteration.

At last, the aggregation of all vultures is carried out by:

$$P(i+1)=\frac{A_1+A_2}{2} \tag{17}$$

Hostile rivalry for Food: When $|F|<0.5$, the leader vultures is starved and frail and do not have adequate power to handle other vultures. The vultures move toward the leader vulture as:

$$P(i+1)=R(i)\left|d(t)\right|\times F\times Levy(d) \tag{18}$$

When $d(t)$ is used in (17), it reflects the space between a vulture and one best vultures in each of the two groups, which is determined using (12). Equation (18) has been improved by employing Levy flight (LF) patterns. LF patterns have been found and exploited in the actions of several search processes, and they have been used to improve the efficacy of the AVOA. The LFs were determined with the help of (19).

$$LF(x)=0.01\times\frac{u+\sigma}{|v|^{\frac{1}{\beta}}},\sigma=\left(\frac{\Gamma(1+\beta)\times\sin\left(\frac{\pi\beta}{2}\right)}{\Gamma(1+\beta_2)\times\beta\times2\left(\frac{\beta-1}{2}\right)}\right)^{\frac{1}{\beta}} \tag{19}$$

Equation (19) denotes the problem dimensions, where d indicates the size of the problem, u and v denote random numbers between zero and one and denote a fixed and default value of 1.5.

B. Pattern Search Algorithm

For solving nonlinear optimization problem, PS algorithm is a powerful tool to obtain local optima from a global solution. The initial value of PS algorithms starts with M_0, and this initial value is provided by the MFO algorithm. In the first iteration, the patterns are created in the form of [0 1], [1 0], [−1 0], and [0 −1]; a lattice point is formed by considering the preliminary point M_0 as $M_0+[0\ 1]$, $M_0+[1\ 0]$, $M_0+[-1\ 0]$, and $M_0+[0\ -1]$. The performance index is measured until it grasps a lesser value than the preliminary value of M_0. This point is termed M_1 which is the preliminary point for the subsequent iteration. Therefore, at the next recapitulation, the lattice point converts $M_1+2*[0\ 1]$, $M_1+2*[1\ 0]$, $M_1+2*[-1\ 0]$, and $M_1+2*[0\ -1]$, and this procedure progresses till the ending criteria are attained. If not satisfied, the initial point can be taken by multiplying a factor of 0.5 known as the contrast factor. So that the lesser performance index is attained and this progression will be recurrent till the end criteria are accomplished.

The flowchart of hybrid AVOA-PS algorithm is shown in Fig. 5.

V. RESULTS AND DISCUSSIONS

A. Application of Hybrid African Vultures Optimization Algorithm-Pattern Search Algorithm

At first, PI controllers are assumed in every area. All the controller values are selected in the limit [−2 to 2]. The system data are

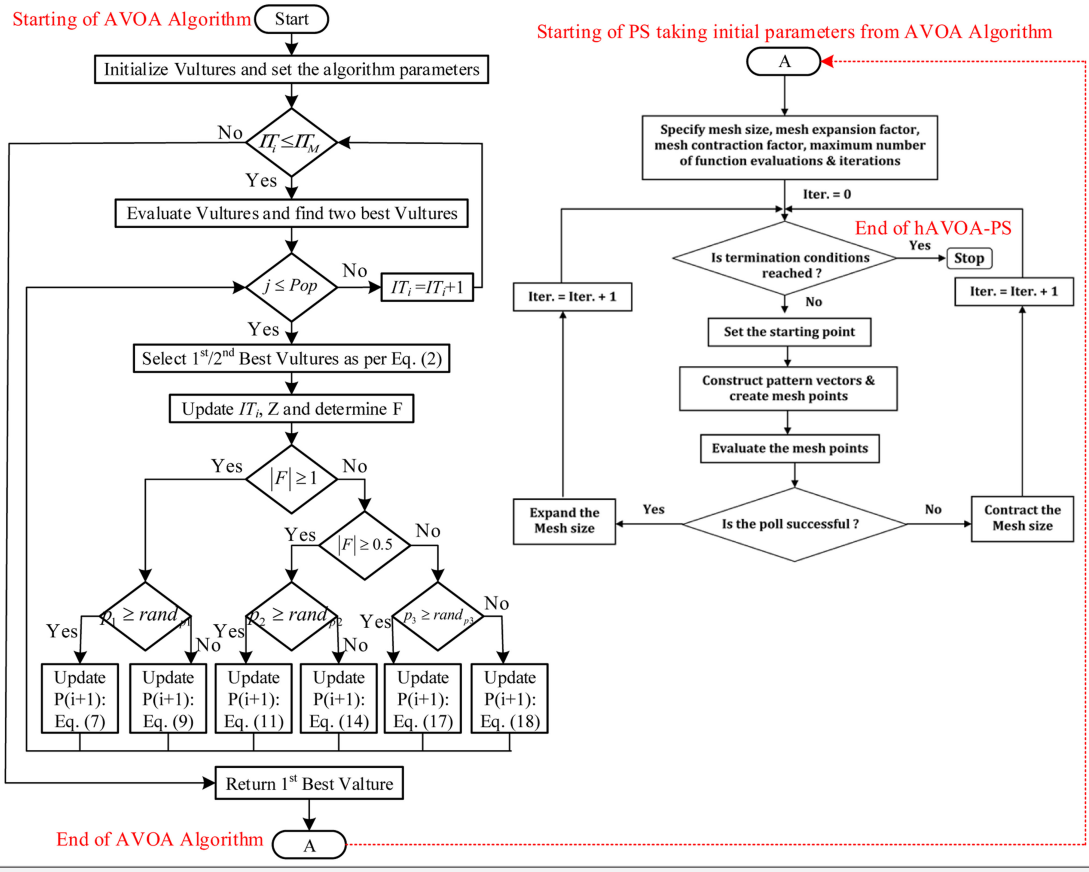

Fig. 5. Flowchart of hAVOA-PS algorithm.

adopted from literature [2]. The test system is simulated by considering a 1% step load increase (SLI) in area 1. To validate the superior performance of hAVOA-PS technique, the PI values are optimized by hAVOA-PS, AVOA, PSO, and GA methods. The algorithms' parameters are given in Table II. For all the methods, 30 search agents and 100 iterations (90 for AVOA and 10 for PS) are taken, and each method is run 30 times. The statistical analysis of studied optimization techniques (GA/PSO/AVOA/hAVOA-PS) with PI structure is presented in Table III. The reported data in Table III indicate that the hAVOA-PS optimization method gives the most excellent result. Moreover, values of maximum and average and standard deviation values with hAVOA-PS are smallest compared to GA/PSO/AVOA. It is clear from Table III that for same PI structure, less $ITAE_{MIN}$ value is attained with AVOA ($ITAE_{MIN}$ = 1.8703) related to GA ($ITAE_{MIN}$ = 2.291) and PSO ($ITAE_{MIN}$ = 1.9974). The $ITAE_{MIN}$ value is reduced to 1.2892 when hAVOAO-PS is engaged. The % reduction in $ITAE_{MIN}$ value with hAVOAO-PS method related to GA, PSO, and AVOA is 43.72%, 35.45%, and 31.06% respectively. The comparison of convergence characteristics of above algorithms is shown in Fig. 6. This authenticates that hAVOAO-PS is superior to AVOA, GA, and PSO.

The optimal results (as per $ITAE_{MIN}$ value) found in 30 runs are selected as controller parameters. The controller values are given in Table IV. The time–domain comparison of techniques with PI controller is revealed in Table V. It can be understood from Table V that the numerical values of S_T, U_S, and O_S in frequency and tie-line responses are least with suggested hAVOA-PS technique related to GA, PSO, and AVOA methods. The $ITAE_{MIN}$ values are further decreased with PID, FPID, and FPID with EV. Table III also reveals that, with the same hAVOAO-PS method, smallest *ITAE* value ($ITAE_{MIN}$= 0.0573) is attained with FPID with EV compared to FPID ($ITAE_{MIN}$= 0.2482) and PID ($ITAE_{MIN}$= 0.5105). The percentage reduction in $ITAE_{MIN}$ with FPID with EV related to PI, PID, and FPID is 95.55%, 88.77%, and 76.91%, respectively.

To measure the controller performance, the following cases are assumed:

Case 1: SLI in area-1
Case 2: Step load decrease (SLD) in all areas
Case 3: SLI in all areas

TABLE II. PARAMETER SETTING OF GA, PSO, AVOA, AND PS ALGORITHMS

Method	Values	Description
GA	Tournament	Selection
	0.9 and 0.1	Crossover and mutation rates
PSO	Reduces from 0.9 to 0.2	Inertia weight, w
	2	Social and cognitive components, c_1 and c_2
AVOA	0.6, 0.4, 0.6	Probability parameters p_1, p_2, p_3
	0.8, 0.6, 2.5	Parameters α, β, γ
PS	1	Mesh size
	2 and 0.5	Mesh expansion and contraction factors

GA, genetic algorithm; PSO, particle swarm optimization; AVOA, African vultures optimization algorithm; PS, pattern search.

TABLE III. STATICAL OUTCOME OF 30 INDEPENDENT RUNS

Technique/Controller	$ITAE_{MIN}$	$ITAE_{MAX}$	$ITAE_{AVE}$	$ITAE_{STD}$
GA/PI	2.2910	3.2002	2.7185	1.652
PSO/PI	1.9974	2.8473	2.2561	1.4824
AVOA/PI	1.8703	2.5439	2.1172	1.2651
hAVOA-PS/PI	1.2892	1.8703	1.5826	0.6272
hAVOA-PS/PID	0.5105	0.7166	0.6127	0.2561
hAVOA-PS/FPID	0.2482	0.3535	0.2952	0.1857
hAVOA-PS/FPID with EV	0.0573	0.0797	0.0615	0.0167

GA, genetic algorithm; PSO, particle swarm optimization; AVOA, African vultures optimization algorithm; hAVOA-PS, hybrid African vultures optimization algorithm and pattern search; PI, proportional integral; EV, electric vehicle; ITAE, integral time absolute error.

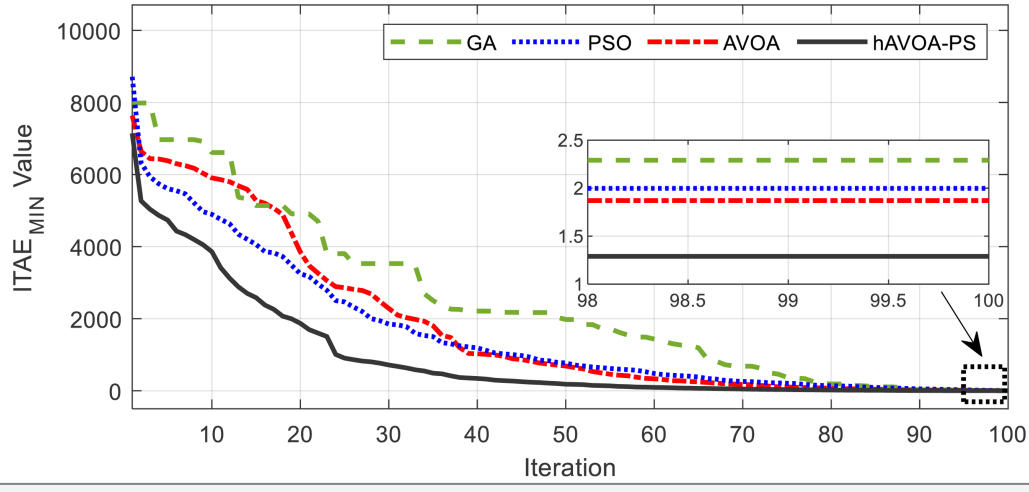

Fig. 6. Comparison of convergence characteristics of GA, PSO, AVOA, and hAVOA-PS.

TABLE IV. OPTIMAL CONTROLLER PARAMETERS

	Area-1	Area-2	Area-3	Area-4	Area-5
GA/PI (K_P, K_I)	0.1280,−0.7459	−0.2621,−0.0821	0.0129,0.2162	−0.1992,−0.8312	−0.8312,−0.7905
PSO/PI (K_P, K_I)	0.1109,−0.6009	0.1507,−0.1343	0.5363,−0.0559	0.2490,0.0649	−0.4701,0.0790
AVOA/PI (K_P, K_I)	−0.1560,0.5205	−0.1182,−0.5079	−0.0769,0.1763	−0.0768,−0.3191	−0.1782,−0.9051
hAVOA-PS/PI (K_P, K_I)	0.2092,−0.3400	0.0063,−0.3702	0.6044,−0.8032	0.2742,−0.4781	−0.1395,−0.2185
hAVOA-PS/PID (K_P, K_I, K_D)	−0.9051,−0.4665 −0.2850	−0.4778,−0.6535 −0.4106	−0.8708, −0.9789 −0.8708	−0.2782, −0.1660 −0.2782	−0.8238, −0.9669 −0.8238
hAVOA-PS/FPID (K_1, K_2, K_P, K_I, K_D)	0.3175,0.3178, −0.4408,−0.7147, −0.0325	0.3174, 0.3176, −0.4561,−0.3726, −0.2299	0.3177,0.3172, −0.0244, −0.3985, −0.0244	0.3178, 0.3175, −0.0244, −0.5618, −0.0244	0.3179, 1.7108, −0.1557, −0.3684, −0.1557
hAVOA-PS/FPID with EV (K_1, K_2, K_P, K_I, K_D)	0.9215, 0.9213 −0.5619,−0.6180, −0.2596	0.9216, 0.9217 −0.0423,−0.1321, −0.1534	0.9211, 0.9218 −0.5176,−0.0212, −0.5176	0.9212, 0.9215 −0.4821, −0.6122, −0.4821	0.9213, 1.3844, −0.2756, −0.0425, −0.2756

GA, genetic algorithm; PSO, particle swarm optimization; AVOA, African vultures optimization algorithm; hAVOA-PS, hybrid African vultures optimization algorithm and pattern search; FPID, fuzzy proportional integral derivative; EV, electric vehicle.

TABLE V. TIME DOMAIN COMPARISON OF TECHNIQUES WITH PI CONTROLLER

Parameter		GA	PSO	AVOA	hAVOA-PS
S_T(s)	ΔF_1	20.52	18.49	16.64	12.14
	ΔF_2	14.41	13.31	11.51	10.18
	ΔF_3	8.69	12.61	8.96	3.13
	ΔF_4	1.82	3.56	3.05	3.23
	ΔF_5	3.0	3.52	3.33	3.33
	ΔP_{Tie1}	18.48	12.46	14.01	7.21
	ΔP_{Tie2}	10.86	7.11	8.58	7.11
	ΔP_{Tie3}	14.31	13.23	12.54	12.34
	ΔP_{Tie4}	11.61	10.24	10.21	10.15
	ΔP_{Tie5}	8.65	8.44	8.37	8.28
U_S (Hz)	ΔF_1	−0.01569	−0.01568	−0.01577	−0.01589
	ΔF_2	−0.00506	−0.00617	−0.00576	−0.00657
	ΔF_3	−0.00388	−0.00401	−0.00399	−0.00438
	ΔF_4	−0.00397	−0.00405	−0.00412	−0.00443
	ΔF_5	−0.00395	−0.00402	−0.00427	−0.00448
U_S (p.u.)	ΔP_{Tie1}	−0.01654	−0.01657	−0.01682	−0.01721
	ΔP_{Tie2}	−0.00326	−0.00211	−0.00265	−0.00215
	ΔP_{Tie3}	−0.00109	−0.00055	−0.00098	−0.00071
	ΔP_{Tie4}	−0.00037	−0.00029	−0.00046	−0.00022
	ΔP_{Tie5}	−0.00050	−0.00026	−0.00038	−0.00019
O_S (Hz)	ΔF_1	0.01208	0.01141	0.01074	0.00961
	ΔF_2	0.00671	0.00415	0.00549	0.00494
	ΔF_3	0.00235	0.00212	0.00248	0.00189
	ΔF_4	0.00161	0.00145	0.00187	0.00168
	ΔF_5	0.00185	0.00164	0.00161	0.00151
O_S (p.u.)	ΔP_{Tie1}	0.00356	0.00308	0.00258	0.00192
	ΔP_{Tie2}	0.00304	0.00267	0.00305	0.00259
	ΔP_{Tie3}	0.00101	0.00101	0.00103	0.00105
	ΔP_{Tie4}	0.00096	0.00096	0.00098	0.00101
	ΔP_{Tie5}	0.00093	0.00093	0.00103	0.00099

PI, proportional integral; GA, genetic algorithm; PSO, particle swarm optimization; AVOA, African vultures optimization algorithm; hAVOA-PS, hybrid African vultures optimization algorithm and pattern search.

Case 4: Large SLI in all areas.
Case 5: Sensitivity analysis.

1) Case 1

A 1% SLI is assumed in area 1. The response with PI controller optimized by different optimization techniques is displayed in Fig. 7. It can be seen from Fig. 7 that, with PI controller, the performance with hAVOAO-PS method is better than GA, PSO, and AVOA methods. This demonstrates the dominance of hAVOAO-PS over AVOA, PSO, and GA.

The system dynamic response with PI, PID, FPID, and FPID with EV for the above disturbance is shown in Fig. 10(F1)-(F10). It is also obvious from Fig. 8(a)-(j) that the responses with FPID controller with EV provide enhanced performance related to FPID, PID, and PI. It is witnessed from results that the numerical values of ITAE, overshoots (Os), and undershoots (Us) due to hAVOAO-PS-optimized FPID with EV are found to be least related to others.

The time domain comparison of techniques with hAVOA-PS technique is presented in Table VI. It can be realized from Table VI that the numerical values of S_T, U_S, and O_S in frequency and tie-line responses are least with suggested FPID+EV compared to PI, OID, and FPID.

2) Case 2

In this case, 4% SLD in areas 1 and 5 and 3% SLD in areas 2, 3, and 4 are assumed. The system dynamic response with PI, PID, and FPID and FPID with EV for the above disturbance is shown in Fig. 9(F1)-(F5). It is also obvious from Fig. 9(F1)-(F5) that the system is unstable with PID controller for the above case and the system stability is preserved with PID and FPID and FPID with EV. However, FPID controller with EV offers improved response than FPID and PID.

3) Case 3

In this case, 2% SLI in areas 1 and 2 and 4% SLI in areas 3, 4, and 5 are assumed. The system dynamic response with PI, PID, and FPID and FPID with EV for the above disturbance is shown in Fig. 10(F1)-(F5). It is also evident from Fig. 10(a)-(e) that the system is unstable with PI and PID controllers for the above case and the system stability is preserved with FPID and FPID with EV. In this case, FPID controller with EV offers improved response than FPID and PID.

4) Case 4

Here, a large SLI of %% is assumed in all the areas. The system response for the above case is shown in Fig. 11(F1)-(F5). It is also evident from Fig. 11(F1)-(F5) that the system is unstable with PI, PID, and FPID controllers for the above case and the system stability is preserved only when FPID with EV is implemented.

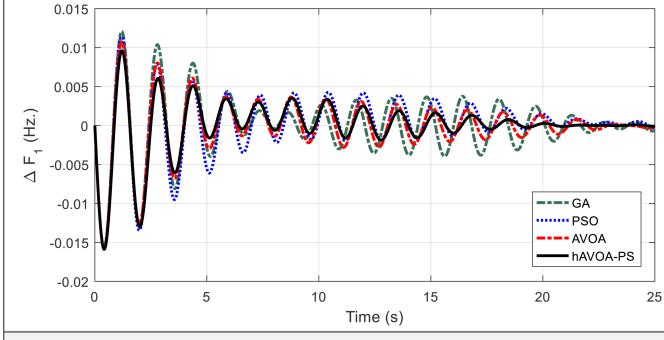

Fig. 7. Case 1: Comparison of techniques with PI controllers.

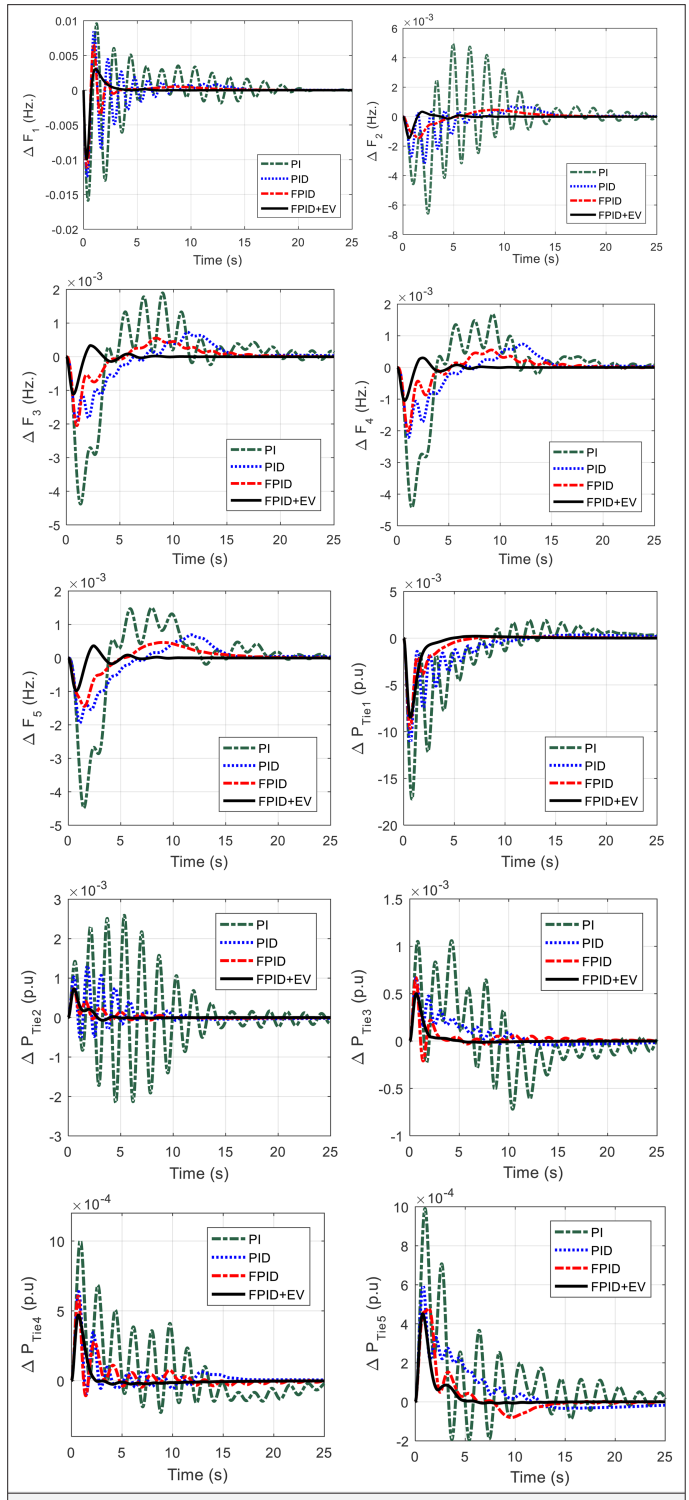

Fig. 8. System response for case 1.

5) Case 5: Sensitivity Analysis

The efficacy of suggested FPIDF+EV control scheme is validated by allowing for variation in system parameters to examine the robustness of the scheme. All the system parameters (gains and time constant) are varied in the range −25% to +25% and the variation in case 4 is simulated. As an example, the response under one variation is shown in Fig. 12, and other results are gathered in Table VII which

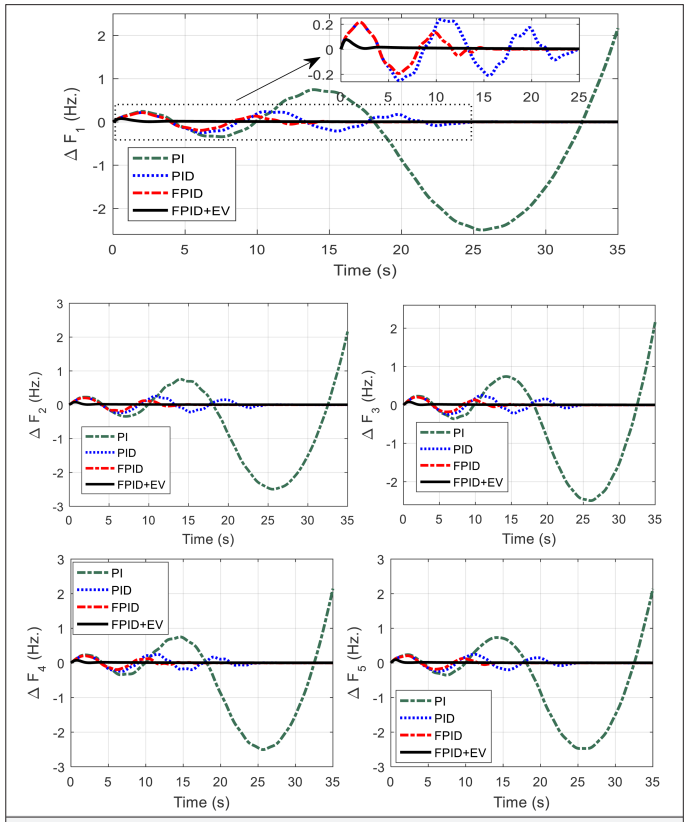

Fig. 9. System response for case 2.

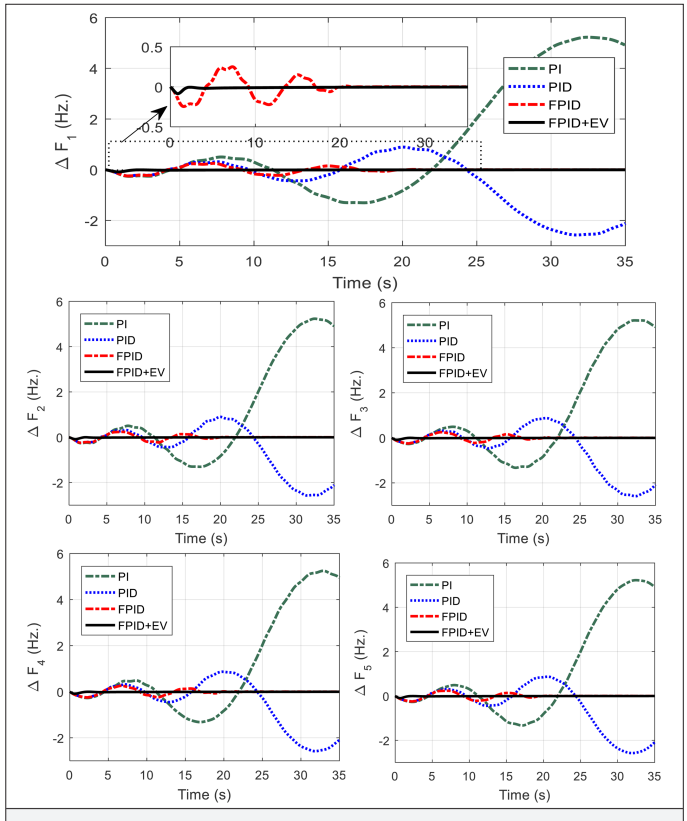

Fig. 10. System response for case 3.

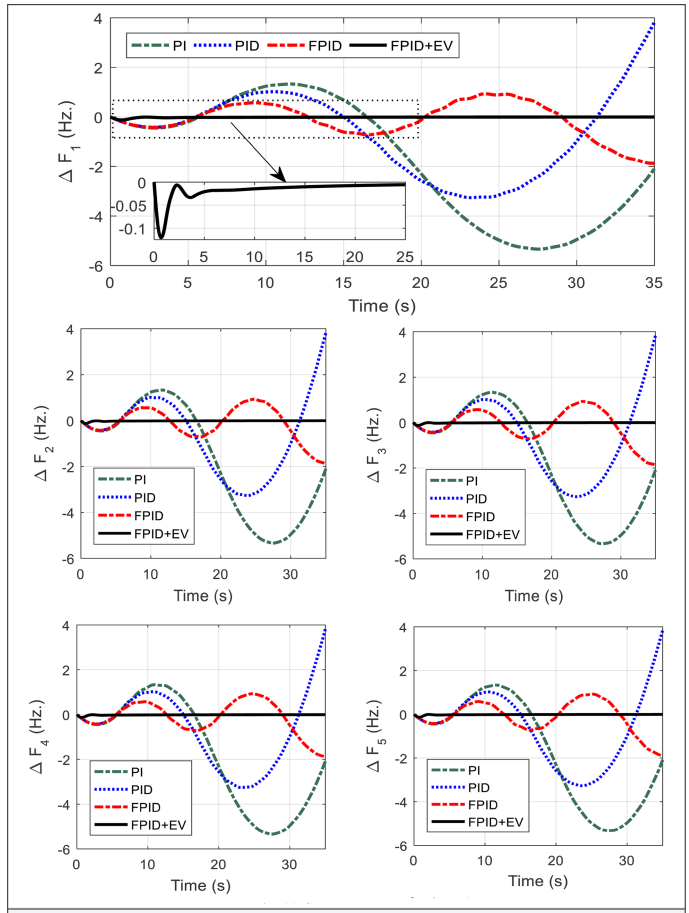

Fig. 11. System response for case 4.

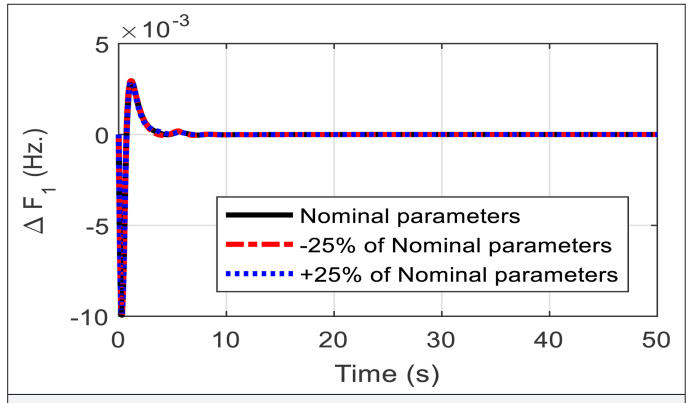

Fig. 12. System response for case 5.

illustrates that the effectiveness of suggested hAVOA-PS-optimized FPIDF+EV frequency control approach as the variations in system performance under parameter variation are insignificant.

B. Comparison with Recent Frequency Control Methods

To demonstrate the advantage of recommended frequency control method, that is, hAVOA-PS optimized FPID controller, a two-area nonreheat thermal power system is taken [25-30]. Two identical FPID controllers are selected in both areas, and hAVOA-PS method is employed to optimize the controllers. The results are:

TABLE VI. COMPARISON OF CONTROLLERS WITH HAVOA-PS TECHNIQUE

Parameter		PI	PID	FPID	FPID+EV
S_T(s)	ΔF_1	12.14	4.28	1.78	1.65
	ΔF_2	10.18	3.52	3.52	0
	ΔF_3	3.13	3.13	1.07	0
	ΔF_4	3.23	1.27	1.09	0
	ΔF_5	3.33	3.33	3.33	0
	ΔP_{Tie1}	7.21	4.28	5.91	1.78
	ΔP_{Tie2}	7.11	6.52	5.45	0
	ΔP_{Tie3}	14.31	13.13	12.63	0
	ΔP_{Tie4}	11.61	11.27	10.27	0
	ΔP_{Tie5}	8.65	7.33	7.25	0
U_S (Hz)	ΔF_1	−0.01589	−0.01241	−0.011105	−0.00993
	ΔF_2	−0.00657	−0.00318	−0.001652	−0.00145
	ΔF_3	−0.00438	−0.00196	−0.00204	−0.00111
	ΔF_4	−0.00443	−0.00221	−0.00201	−0.00105
	ΔF_5	−0.00448	−0.00194	−0.00144	−0.00098
U_S (p.u.)	ΔP_{Tie1}	−0.01721	−0.01117	−0.00966	−0.00851
	ΔP_{Tie2}	−0.00215	−0.00054	−0.00006	−0.000076
	ΔP_{Tie3}	−0.00071	−0.00004	−0.000209	−0.000014
	ΔP_{Tie4}	−0.00022	−0.00009	−0.000108	−0.000029
	ΔP_{Tie5}	−0.00019	−0.000033	−0.00008	−0.000007
O_S (Hz)	ΔF_1	0.00961	0.00857	0.00663	0.00295
	ΔF_2	0.00494	0.00068	0.00058	0.000346
	ΔF_3	0.00189	0.00073	0.00055	0.00033
	ΔF_4	0.00168	0.00074	0.00055	0.00031
	ΔF_5	0.00151	0.00069	0.00046	0.00037
O_S (p.u.)	ΔP_{Tie1}	0.00192	0.00034	0.00013	0.00021
	ΔP_{Tie2}	0.00259	0.0013	0.00073	0.00072
	ΔP_{Tie3}	0.00105	0.00067	0.00066	0.000502
	ΔP_{Tie4}	0.00101	0.00063	0.00061	0.00047
	ΔP_{Tie5}	0.00099	0.00059	0.00048	0.00045

PID, proportional integral derivative; FPID, fuzzy PID, proportional integral derivative; PI, proportional integral; EV, electric vehicle.

$K_1 = 0.9981$, $K_2 = 0.0012$, $K_P = 1.6556$, $K_I = 1.9742$, $K_D = 0.5105$

At t = 0 seconds, a 10% SLI is assumed in area 1. The performances of hAVOA-PS optimized FPID are equated with TLBO-optimized 2DOFPID [25], JA-optimized PIDN [26], BFOA-tuned PI [27], GA-optimized PI [28], hBFOA-PSO-tuned PI [29], and hPSO-PS-optimized FPI [30]. The dynamic result is depicted in Fig. 13 which confirms that the suggested method outperforms the published approaches.

C. Comparison with OPAL-RT results

The MATLAB outcomes are related to OPAL-RT results for authentication of the suggested method as depicted in Fig. 14. The OPAL-RT method emulates the delays and errors that are inherently

TABLE VII. SENSITIVITY ANALYSIS WITH HAVOA-PS OPTIMIZED CONTROLLER (FPID+EV)

Parameter		−25%	+25%	Parameter		−25%	+25%
S_T(s)	ΔF_1	1.6600	1.6300	U_S (p.u.)	ΔP_{Tie1}	−0.0083	−0.0085
	ΔF_2	0	0		ΔP_{Tie2}	−0.0001	−0.0001
	ΔF_3	0	0		ΔP_{Tie3}	0	0
	ΔF_4	0	0		ΔP_{Tie4}	0	0
	ΔF_5	0	0		ΔP_{Tie5}	0	0
	ΔP_{Tie1}	1.71	1.84	O_S (Hz)	ΔF_1	0.003	0.0029
	ΔP_{Tie2}	0	0		ΔF_2	0.0004	0.0003
	ΔP_{Tie3}	0	0		ΔF_3	0.0004	0.0003
	ΔP_{Tie4}	0	0		ΔF_4	0.0004	0.0002
	ΔP_{Tie5}	0	0		ΔF_5	0.0005	0.0003
U_S (Hz)	ΔF_1	−0.0100	−0.0099	O_S (p.u.)	ΔP_{Tie1}	0.0002	0.0002
	ΔF_2	−0.0016	−0.0013		ΔP_{Tie2}	0.0007	0.0007
	ΔF_3	−0.0014	−0.0010		ΔP_{Tie3}	0.0005	0.0005
	ΔF_4	−0.0013	−0.0009		ΔP_{Tie4}	0.0004	0.0005
	ΔF_5	−0.0012	−0.0008		ΔP_{Tie5}	0.0005	0.0005

FPID, fuzzy PID, proportional integral derivative; hAVOA-PS, hybrid African vultures optimization algorithm and pattern search; EV, electric vehicle.

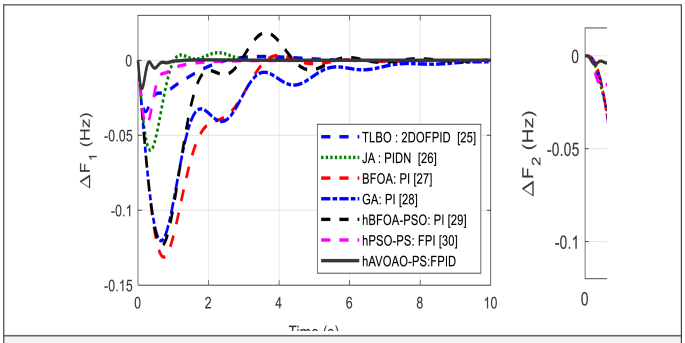

Fig. 13. Comparison with recent frequency control approaches.

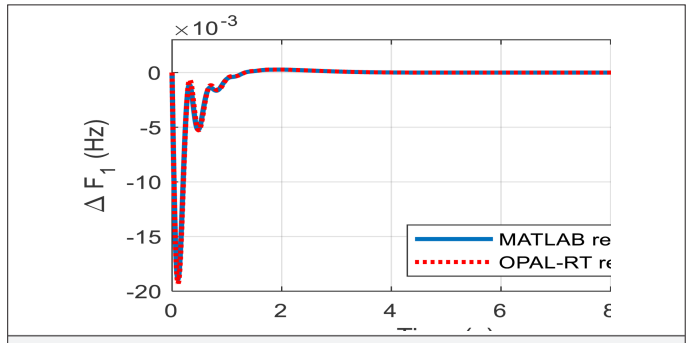

Fig. 14. Comparison of MATLAB and OPAL-RT results.

present but ignored in the MATLAB simulations. The frequency change responses of MATLAB/SIMULINK and OPAL-RT-based real-time simulator (RTS) for five area and two area are shown in Fig. 14 from which it can be seen that MATLAB/SIMULINK outcomes match with OPAL-RT results.

VI. CONCLUSIONS

An optimization method by hybridizing AVOA and PS (hAVOA-PS) is projected to optimize the FPID parameters for frequency control of a five-area nonlinear power system in the presence of EVs. Initially, a five-area system without EV is assumed and the PI parameters are tuned by GA, PSO, AVOA, and proposed hAVOA-PS methods. It is found that the % decrease in *ITAE* value with hAVOAO-PS method related to GA, PSO, and AVOA is 43.72%, 35.45%, and 31.06%, respectively. In the next stage, PID and FPID controllers are considered and EVs are included in each area. It is noticed that, with the same hAVOAO-PS technique, the % decrease in *ITAE* value with FPID with EV related to PI, PID, and FPID is 95.55%, 88.77%, and 76.91%, respectively. To exhibit the effectiveness of projected frequency control scheme, different cases like SLI in area-1 only, SLD in all areas, SLI in all areas, and large SLI in all areas are considered. It is observed that the FPID with EV frequency control approach is able to preserve system stability for all the cases whereas other compared approaches fail to maintain stability in some cases. It is observed that:

- hAVOA-PS technique provides superior results compared to AVOA, PSO, and GA methods.
- hAVOA-PS-optimized FPID+EV control scheme provides better frequency regulation compared to FPID and PID controllers.
- The proposed control scheme is robust and retuning is not required when the system parameters change.

- The proposed control approach provides improved frequency regulation compared to some recently proposed approaches in a standard test system.
- The proposed control scheme can be employed for real-time implementation as MATLAB results are closely matching with the OPAL-RT results.

As a future study, the current work can be extended to a large system including unpredictable wind and solar energies.

Peer-review: Externally peer-reviewed.

Author Contributions: Concept – S.K.M.; Design – S.K.M.; Supervision – P.M.D., A.K.B.; Materials – P.M.D., A.K.B.; Data Collection and/or Processing – P.M.D., S.K.M.; Analysis and/or Interpretation – S.K.M., P.M.D.; Literature Review – P.M.D., A.K.B.; Writing – S.K.M., P.M.D.; Critical Review – S.K.M., A.K.B.

Declaration of Interests: The authors have no conflicts of interest to declare.

Funding: The authors declared that this study has received no financial support.

REFERENCES

1. O. I. Elgerd, and C. E. Fosha, "Optimum megawatt-frequency control of multiarea electric energy systems," *IEEE Trans. Power Apparatus Syst.*, vol. PAS–89, no. 4, pp. 556–563, 1970. [CrossRef]
2. L. C. Saikia, J. Nanda, and S. Mishra, "Performance comparison of several classical controllers in AGC for multi-area interconnected thermal system," *Int. J. Electr. Power Energy Syst.*, vol. 33, no. 3, pp. 394–401, 2011. [CrossRef]
3. S. Mishra, R. C. Prusty, and S. Panda, "Design and analysis of 2dof-PID controller for frequency regulation of multi-microgrid using hybrid dragonfly and pattern search algorithm," *J. Control Autom. Electr. Syst.*, vol. 31, no. 3, pp. 813–827, 2020. [CrossRef]
4. A. Kumar, R. K. Khadanga, and S. Panda, "Reinforced modified equilibrium optimization technique-based MS-PID frequency regulator for a hybrid power system with renewable energy sources," *Soft Comput.*, vol. 26, no. 11, 5437–5455, 2022. [CrossRef]
5. R. K. Khadanga, A. Kumar, and S. Panda, "A novel sine augmented scaled sine cosine algorithm for frequency control issues of a hybrid distributed two-area power system," *Neural Comput. Appl.*, vol. 33, no. 19, pp. 12791–12804, 2021. [CrossRef]
6. P. C. Nayak, U. C. Prusty, R. C. Prusty, and S. Panda, "Imperialist competitive algorithm optimized cascade controller for load frequency control of multi-microgrid system," *Energy Sources A*, 2021. [CrossRef]
7. P. C. Nayak, S. Mishra, R. C. Prusty, and S. Panda, "Performance analysis of hydrogen aqua equalizer fuel-cell on AGC of Wind-hydro-thermal power systems with sunflower algorithm optimized fuzzy-PDFPI controller," *Int. J. Ambient Energy*, vol. 43, pp. 1–14, 2020.
8. P. C. Nayak, B. P. Nayak, R. C. Prusty, and S. Panda, "Sunflower optimization based fractional order fuzzy PID controller," *Energy Sources, Part A: Recovery, Utilization, and Environmental Effects*, pp. 1–20, 2021.
9. B. K. Sahu, S. Pati, and S. Panda, "Hybrid differential evolution particle swarm optimisation optimised fuzzy proportional–integral derivative controller for automatic generation control of interconnected power system," *IET Gener. Transm. Distrib.*, vol. 8, no. 11, pp. 1789–1800, 2014. [CrossRef]
10. D. Guha, P. K. Roy, and S. Banerjee, "Quasi-oppositional JAYA optimized 2-degree-of-freedom PID controller for load-frequency control of interconnected power systems," *Int. J. Simul. Modell.*, vol. 15, pp. 1–23, 2020.
11. B. Khokhar, S. Dahiya, and K. P. S. Parmar, "Load frequency control of a microgrid employing a 2D Sine Logistic map based chaotic sine cosine algorithm," *Appl. Soft Comput.*, vol. 109, p. 107564, 2021. [CrossRef]
12. K. Peddakapu, M. R. Mohameda, P. Srinivasarao, and P. K. Leung, "Frequency stabilization in interconnected power system using bat and harmony search algorithm with coordinated controllers," *Appl. Soft Comput.*, vol. 113, p. 107986, 2021. [CrossRef]
13. A. A. A. El-Ela, R. A. El-Sehiemy, A. M. Shaheen, and A. E. Diab, "Design of cascaded controller based on coyote optimizer for load frequency control in multi-area power systems with renewable sources," *Control Eng. Pract.*, vol. 121, p. 105058, 2022. [CrossRef]
14. A. X. R. Irudayaraj et al., "Renewable sources-based automatic load frequency control of interconnected systems using chaotic atom search optimization," *Appl. Soft Comput.*, vol. 119, 2022. [CrossRef]
15. H. Shayeghi, A. Rahnama, and H. H. Alhelou, "Frequency control of fully-renewable interconnected microgrid using fuzzy cascade controller with demand response program considering," *Energy Rep.*, vol. 7, pp. 6077–6094, 2021. [CrossRef]
16. S. Padhy, and S. Panda, "Application of a simplified Grey Wolf optimization technique for adaptive fuzzy PID controller design for frequency regulation of a distributed power generation system," *Prot. Control Mod. Power Syst.*, vol. 6, pp. 1–6, 2021.
17. Y. Arya, and N. Kumar, "Fuzzy gain scheduling controllers for automatic generation control of two-area interconnected electrical power systems," *Electr. Power Compon. Syst.*, vol. 44, no. 7, pp. 737–751, 2016. [CrossRef]
18. G. Sharma , A. Panwar, Y. Arya, and M. Kumawat, "Integrating layered recurrent ANN with robust control strategy for diverse operating conditions of AGC of the power system," *IET Gener. Transm. Distrib.*, vol. 14, No. 18, pp. 3886–3895, 2020. [CrossRef]
19. M. Sharma, S. Dhundhara, Y. Arya, and S. Prakash, "Frequency stabilization in deregulated energy system using coordinated operation of fuzzy controller and redox flow battery,", *Int. J. Energy Res.*, vol. 45, No. 5, pp. 7457–7475, 2021. [CrossRef]
20. M. Sharma, S. Dhundhara, Y. Arya, and S. Prakash, "Frequency excursion mitigation strategy using a novel COA optimised fuzzy controller in wind integrated power systems," *IET Renew. Power Gener.*, vol. 14, No. 19, pp. 4071–4085, 2020. [CrossRef]
21. R. Pilla, N. Botcha, T. S. Gorripotu, and A. T. Azar, "Fuzzy PID controller for automatic generation control of interconnected power system tuned by glow-worm swarm optimization," In *ARIAM 2019. Learning and Analytics in Intelligent Systems, Applications of Robotics in Industry Using Advanced Mechanisms*, Vol. 5. Cham: Springer, 2020, 140–149. [CrossRef]
22. P. K. Mohanty, B. K. Sahu, T. K. Pati, S. Panda, and S. K. Kumar Kar, "Design and analysis of fuzzy PID controller with derivative filter for AGC in multi-area interconnected power system,", *IET Generation Transmission & Distribution*, vol. 10, No. 15, pp. 3764–3776, 2016. [CrossRef]
23. A. K. Barik, D. Tripathy, D. C. Das, and S. C. Sahoo, "Optimal load-frequency regulation of demand response supported isolated hybrid microgrid using fuzzy Pd+I controller," In *ICIMSAT 2019. Learning and Analytics in Intelligent Systems, Intelligent Techniques and Applications in Science and Technology*, Vol. 12. Cham: Springer, 2020, 798–806. [CrossRef]
24. B. Abdollahzadeh, F. S. Gharehchopogh, and S. Mirjalili, "African vultures optimization algorithm: A new nature-inspired metaheuristic algorithm for global optimization problems," *Comput. Ind. Eng.*, vol. 158, p. 107408, 2021. [CrossRef]
25. R. K. Sahu, S. Panda, U. K. Rout, and D. K. Saho, "Teaching learning based optimization algorithm for automatic generation control of power system using 2-dof PID controller, Electrical," *J. Power Energy Syst.*, vol. 77, pp. 287–301, 2016.
26. S. P. Singh, T. Prakash, V. P. Singh, and M. G. Babu, "Analytic hierarchy process based automatic generation control of multi-area interconnected power system using Jaya algorithm," *Eng. Appl. Artif. Intell.*, vol. 60, pp. 35–44, 2017. [CrossRef]
27. E. S. Ali, and S. M.Abd-Elazim, "Bacteria foraging optimization algorithm based load frequency controller for interconnected power system," *Int. J. Electr. Power Energy Syst.*, vol. 33, no. 3, pp. 633–638, 2011. [CrossRef]
28. Y. L. Abdel-Magid, and M. M. Dawoud, "Optimal AGC tuning with genetic algorithms," *Electr. Power Syst. Res.*, vol.38, no. 3, pp. 231–238, 1996. [CrossRef]
29. S. Panda, B. Mohanty, and P. K. Hota, "Hybrid BFOA-PSO algorithm for automatic generation control of linear and nonlinear interconnected power systems," *Appl. Soft Comput.*, vol. 13, no. 12, pp. 4718–4730, 2013. [CrossRef]
30. R. K. Sahu, S. Panda, and G. T. C. Sekhar, "A novel hybrid PSO – PS optimized fuzzy PI controller for AGC in multi area interconnected power systems," *Int. J. Electr. Power Energy Syst.*, vol. 64, pp. 880–893, 2015. [CrossRef]

Mr. Pabitra Mohan Dash graduated in Electrical Engineering in 1993, M.Tech Degree in Electrical Engineering in 2008, and currently, he is working as Associate Professor in Electrical Engineering, Bhubaneswar Engineering College, Bhubaneswar, Odisha, and Research scholar under BPUT, Odisha. His research interests are the field of electrical power system and control, optimization techniques, flexible AC transmission controller, and load frequency control.

Dr. Sangram Keshori Mohapatra received BE degree in Electrical Engineering in the year 1999, M.Tech degree in the year of 2008 in the specialization of Power Electronics and Drives, and Ph.D. degree in the year of 2014 in the specialization of power system Engineering. He has acquired more than 22 years of experience in the field of academics and research pertaining to Electrical Engineering. Presently, he is working as an Associate Professor in Electrical Engineering, Government College of Engineering, Keonjhar, a constituent college of BPUT, Odisha. He has published about 60 papers in international journal and conferences. He has guided 25 M.Tech research scholars .He is currently guiding 4 Ph.D. research scholars. He is the life member of Indian Society for Technical Education (ISTE), India and Fellow of The Intuitions of Engineers (IEI), and member of IEEE and reviewer of various reputed journals. His research interest is in the area of flexible AC transmission systems (FACTS), modeling of machines, power electronics, power systems and FACTS, controller design, power system stability, optimization Techniques, and Automatic generation and control.

Dr. Asini Kumar Baliarsingh rewceived B.E. degree in Electrical Engineering from Utkal University in 1998, M.Tech degree in 2004 from NIT, Jamesdpur, India. He received the Ph.D. degree in the year 2012. He is currently working in Electrical Engineering Department in Government College of Engineering, Kalahandi, Odisha, India. He has published more than 40 papers in International Journal and Conferences. He has more than 22-year experience in teaching and research experience in the field of Electrical Engineering. He is member of ISTE, India. His research interests are in FACTS Controller, AI techniques, power system stability problem, etc.